

Spectral evidence for Dirac spinons in a kagome lattice antiferromagnet

Zhenyuan Zeng,^{1,2} Chengkang Zhou,³ Honglin Zhou,^{1,2} Lankun Han,^{1,2} Runze Chi,^{1,2} Kuo Li,⁴ Maiko Kofu,⁵ Kenji Nakajima,^{5,*} Yuan Wei,⁶ Wenliang Zhang,⁶ Daniel G. Mazzone,⁷ Zi Yang Meng,^{3,†} and Shiliang Li^{1,2,8,‡}

¹*Beijing National Laboratory for Condensed Matter Physics,*

Institute of Physics, Chinese Academy of Sciences, Beijing 100190, China

²*School of Physical Sciences, University of Chinese Academy of Sciences, Beijing 100190, China*

³*Department of Physics and HKU-UCAS Joint Institute of Theoretical and Computational Physics,
The University of Hong Kong, Pokfulam Road, Hong Kong SAR, China*

⁴*Center for High Pressure Science and Technology Advanced Research,
10 Xibeiwang East Road, Haidian, Beijing 100094, China*

⁵*J-PARC Center, Japan Atomic Energy Agency, Tokai, Ibaraki, 319-1195, Japan*

⁶*Photon Science Division, Paul Scherrer Institut, CH-5232 Villigen PSI, Switzerland*

⁷*Laboratory for Neutron Scattering and Imaging,*

Paul Scherrer Institut, CH-5232 Villigen PSI, Switzerland

⁸*Songshan Lake Materials Laboratory, Dongguan, Guangdong, 523808, China*

Emergent quasiparticles with a Dirac dispersion in condensed matter systems can be described by the Dirac equation for relativistic electrons, in analogy with Dirac particles in high-energy physics. For example, electrons with a Dirac dispersion have been intensively studied in electronic systems such as graphene and topological insulators. However, charge is not a prerequisite for Dirac fermions, and the emergence of Dirac fermions without charge degree of freedom has been theoretically predicted to be realized in Dirac quantum spin liquids. These quasiparticles carry a spin of $1/2$ but are charge-neutral, and so are called spinons. Here we show that the spin excitations of a kagome antiferromagnet, $\text{YCu}_3(\text{OD})_6\text{Br}_2[\text{Br}_{0.33}(\text{OD})_{0.67}]$, are conical with a spin continuum inside, which is consistent with the convolution of two Dirac spinons. The predictions of a Dirac spin liquid model with a spinon velocity obtained from the spectral measurements are in agreement with the low-temperature specific heat of the sample. Our results thus provide spectral evidence for the Dirac quantum spin liquid state emerging in this kagome lattice antiferromagnet. However, the locations of the conical spin excitations differ from those calculated by the nearest neighbor Heisenberg model, suggesting the Dirac spinons have an unexpected origin.

Quantum spin liquids (QSLs) provide an ideal platform for realizing quantum states of matter beyond the Landau paradigm of symmetry and its spontaneous breaking [1–4]. One of the crucial features of QSLs is the presence of fractionalized excitations, which have the form of elemental quasiparticles carrying the topological nature and interacting with the emergent gauge field [5–10]. Spinons are fractionalized excitations in the sense that they carry a spin of $1/2$ but are charge-neutral. The spinons can be gapped or gapless. In the gapless state, the spinons can have a conical shape dispersion with the apex located at zero energy. This spectrum is like that of the Dirac cones in the electronic band structures of graphene and topological insulators [11–13]. Therefore, the spinons in Dirac QSLs are a new kind of Dirac quasiparticle without the charge degree of freedom. Although a Dirac QSL is interesting in its own right, it also serves as the parent state of novel two-dimensional quantum phases characterized by emergence and deconfinement [14–17]. Although Dirac QSLs have been highly anticipated in many theoretical models of different kinds of lattices [18–32], their material realization has remained elusive due to the lack of spectral evidence.

Although it is hard to directly detect single spinon excitations, two spinon excitations with total spin quantum number $S = 1$ can result in a spin continuum that can be

revealed by inelastic neutron scattering (INS). For Dirac spinons, one would expect that the spin excitations exhibit a convolved cone structure with a finite and continuous spectral weight inside the cone (unlike the spin wave of linear dispersing magnons that have no weight inside the cone) and with an apex at zero energy with respect to the ground state of the spin system [31, 32], as illustrated in Fig. 1a. In materials that have been theoretically suggested to host Dirac QSLs [20, 27, 29], the spin excitations observed in the INS experiments either do not look like Dirac spinons or are too blurry for their nature to be determined [34–37].

The discovery in this work changes the situation. The material studied in this work is $\text{YCu}_3(\text{OH})_6\text{Br}_2[\text{Br}_{1-x}(\text{OH})_x]$ (denoted as $\text{YCu}_3\text{-Br}$ hereafter). It has perfect kagome planes formed by Cu^{2+} ions with $S = 1/2$ [38]. Previous measurements have shown that there is no magnetic ordering down to 50 mK although its Weiss temperature is about -80 K [39–42]. Moreover, the low-temperature specific heat shows a T^2 dependence at zero field and a T -linear term under a field [39], which is consistent with a Dirac QSL [20]. Indeed, our neutron scattering results presented in this work for $\text{YCu}_3\text{-Br}$ ($x = 0.67$) clearly reveal six conical spin excitations with filled continuum weights inside the cones (Fig. 1b and 1d). This represents strong evidence that the

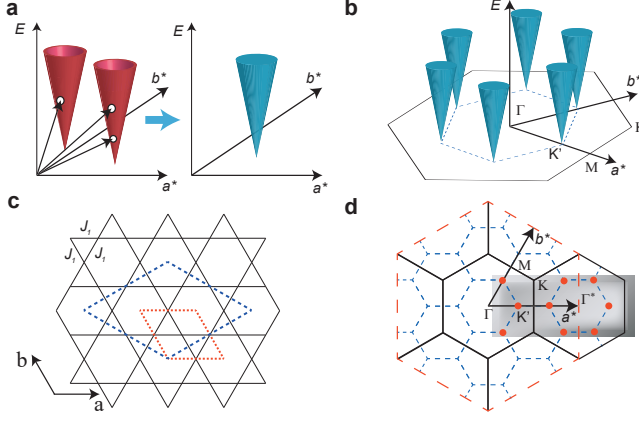


FIG. 1. Schematics of the low-energy conical spin excitations and reciprocal space for YCu₃-Br. **a**, Schematic illustration of two Dirac spinons with a conical-surface dispersion (red) that merged into a cone spin excitations with continuum inside (blue). The two spinons can come from either two different Dirac cones or the same one as indicated by the white dots. **b**, Six conical low-energy spin excitations in YCu₃-Br. Their momenta in the kagome Brillouin zone is indicated. **c**, The in-plane kagome structure. The dashed red and blue lines represent the lattice unit cell of YCu₃-Br and Y₃Cu₉(OH)₁₉Cl₈ [33], respectively. **d**, Sketch of the in-plane reciprocal space. The black solid line and the red and blue dashed lines represent the kagome, the extended kagome and the lattice of the Y₃Cu₉(OH)₁₉Cl₈ Brillouin zones, respectively. The gray shaded area illustrates the regime measured in this work.

material realizes the long-sought-after Dirac QSL.

Figures 2a-2d show contour plots of the in-plane low-energy excitations at several energies at 0.3 K for the deuterated YCu₃-Br. Six symmetrical spin excitations are centered at $(1, 0)$ in the second Brillouin zone. The positions are at $(2/3, 0)$ and the corresponding six-fold rotational points about the c^* -axis at $(1, 0)$. Note that these positions correspond to the K' points in Fig. 1d. The peaks at 0.2 meV in Fig. 2a are sharp and elongated along the direction vertical to Q due to sample mosaic. With increasing energy (Fig. 2b to Fig. 2d), the peaks become broader, but no ring-like structure is observed at any energy and the excitations are always continuum with filled cones. Figure 2e shows an $E - Q$ plot with Q along the $[H, 0]$ direction. One can clearly see two filled cone-like excitations at $(2/3, 0)$ and $(4/3, 0)$, which disappear at 30 K (Fig. 2f), confirming the magnetic origin of these excitations.

To further quantitatively analyze the data, we made a cut along the $[H, 0]$ direction at 0.2 meV, as shown in Fig. 3a. Besides the peaks at $(2/3, 0)$ and $(4/3, 0)$, there is also a peak at $(1/3, 0)$. This suggests that the spin excitations also exist at the first Brillouin zone of the kagome lattice. Figure 3b shows the integrated intensity of the peaks normalized by the magnetic form factor as a function of the in-plane $|Q_{in}| = |[H, K]|$. The integrated in-

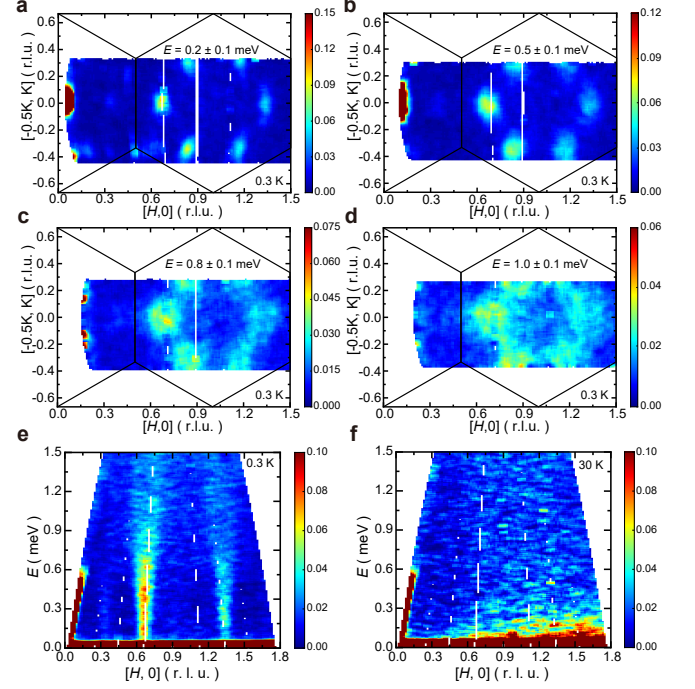


FIG. 2. INS results at low energies with $E_i = 2.566$ meV. **a-d**, Intensity contour plots of the INS results at 0.3 K in the $[H, K]$ zone at 0.2 meV (**a**), 0.5 meV (**b**), 0.8 meV (**c**) and 1 meV (**d**). The \pm sign gives the integrated energy range. The solid lines forming the hexagons mark the kagome Brillouin zones. The x and y axes are the components of Q parallel to $(H, 0)$ and $(-0.5K, K)$, respectively. The positions of the excitations are at $(1 \pm 1/3, 0)$, $(1, \pm 1/3)$ and $(1 \pm 1/3, \mp 1/3)$. **e, f**, Intensity contour plots of the INS results as a function of E and Q along the $[H, 0]$ direction at 0.3 K (**e**) and 30 K (**f**). The integrated range along the $[-K/2, K/2]$ is from $K = -0.05$ to $K = 0.05$.

tensity is fitted well by $A(1 - \cos(\pi|Q_{in}|/|Q_{(1,0)}|))$, where A is the only fitting parameter. This function explains why the intensity of the $(1/3, 0)$ peak is much weaker and resembles the structure factor of randomly arranged nearest-neighbour singlets [34]. In a similar system with long-range antiferromagnetic order [33], the spin excitations are also very strong in the second kagome Brillouin zone. Whether the fitting observed in Fig. 3b is coincidental or has a deeper physical meaning warrants further theoretical investigation. It is important to emphasize that the spin excitations around the peak positions do not follow the structure factor of randomly arranged nearest-neighbour singlets but exhibit a lorentzian behavior, as described below. Figure 3c shows the Q -cuts along the $[H, 0]$ direction at $(2/3, 0)$, which can all be well fitted by the Lorentzian function. The fitted full-width at half-maximum (FWHM) at 0.12 meV is about $0.035 \pm 0.007 \text{ \AA}^{-1}$, which corresponds to a spin-spin correlation of about 180 \AA without considering the instrumental resolution. Moreover, the FWHM shows linear dependence below 0.6 meV (Fig. 3d), which has a slope and intercept

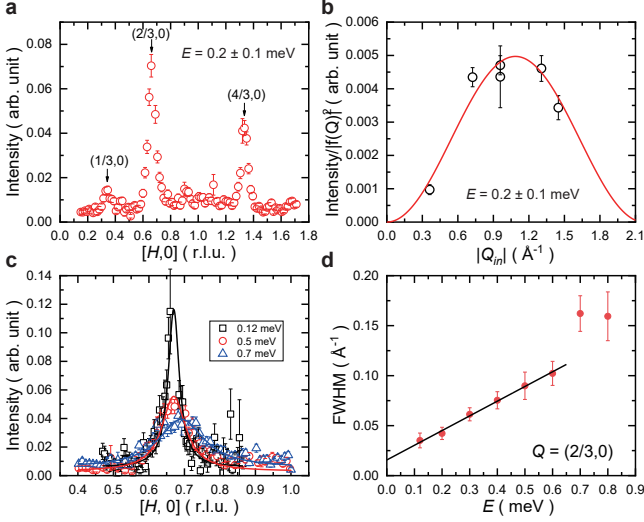


FIG. 3. **Quantitatively analysis for the low-energy data at 0.3 K.** **a**, Constant- E cuts along the $[H, 0]$ direction at 0.2 meV. **b**, The in-plane $|Q_{in}|$ dependence of the integrated intensity of the peaks at 0.2 meV, which has been normalized to the square of the magnetic form factor of the Cu^{2+} ion. The solid line is the fit to a cosine function, as described in the main text. **c**, Constant- E cuts along the $[H, 0]$ direction at several energies near $(2/3, 0)$. The solid lines are fits to the Lorentzian function. **d**, The energy dependence of the FWHM at $Q = (2/3, 0)$. The solid line is a linear fit. The error bars in all the panels represent one-standard-deviation uncertainty in the data based on Poisson statistics with the sample size being the neutron counts.

of $0.147 \text{ \AA}^{-1}/\text{meV}$ and 0.016 \AA^{-1} , respectively. Note that the latter is very close to the instrumental resolution [43]. The slope provides information about the velocity of spinons ν_F if the cone spin excitations come from the convolution of two Dirac spinons. The value is about $1 \times 10^3 \text{ m/s}$ for free spinons and there could be renormalization due to interaction effects and the detailed fusion behaviour of two spinons.

The high-energy spin excitations of $\text{YCu}_3\text{-Br}$ are shown in Fig. 4. At 1.3 meV, the excitations become so broad that they seem to be connected with those in adjacent zones (Fig. 4a). With increasing energy, the jointed six-branches spin excitations merge into one centered around $(1, 0)$ and the area becomes smaller with increasing energy, as shown in Fig. 4b - 4d. The top of the excitations ends at about 7.5 meV (Fig. 4e), which is about 100 times the lowest energy observed. Unlike the low-energy spin excitations, the high-energy spin excitations survive at 30 K although there is substantial broadening (Fig. 4f).

As we can observe the whole spectra within the second kagome Brillouin zone, the static susceptibility $\chi'(Q, 0)$ can be obtained from the imaginary part of the dynamical

susceptibility $\chi''(Q, \omega)$ by the Kramers-Kronig relation,

$$\chi'(Q, 0) \propto \int_{-\infty}^{\infty} \frac{\chi''(Q, \omega)}{\omega} d\omega. \quad (1)$$

According to the fluctuation-dissipation theorem, we have $\chi''(Q, \omega) = S(Q, \omega) \times [1 - \exp(-\hbar\omega/k_B T)]$, where $S(Q, \omega)$ is the scattering function that is proportional to the signal obtained from the INS measurements. Moreover, as $\chi''(Q, \omega)$ is the odd function of the energy, the integral can be done by just considering $S(Q, \omega)$ at positive energy. The calculated result is shown in Fig. 4g, where there are still six symmetrical peaks. Figure 4h shows the H -cut at the $(4/3, 0)$ peak and its Lorentzian fit. The magnetic correlation length ξ is thus calculated to be about 83 \AA without considering the instrumental resolution, which is about 25 Cu-Cu bond lengths.

Our results provide strong evidence for an emerging Dirac QSL state in $\text{YCu}_3\text{-Br}$. The key finding in our work is the low-energy conical spin excitations with continuum inside, which requires a non-trivial origin of the low-energy excitations. For the conical spin excitations, trivial explanations such as damped spin waves in the presence of strong disorders cannot simultaneously reproduce the sharp excitations near zero energy and broad spectra at higher energies [43]. The low-energy spinon continuum due to strong disorders always extend to a large area in the momentum space at low energies since disorder tends to destroy the spin-spin correlation and always reduces the spin-spin correlation length [44–48]. In contrast, these features can be explained well by the presence of Dirac spinons, which results in conical spin excitations by two-spinon convolution [20]. The picture based on Dirac spinons also gives us a quantitative comparison between the INS and specific-heat measurements. According to a previous report [39], the low-temperature specific heat of $\text{YCu}_3\text{-Br}$ exhibits a quadratic temperature dependence at zero field, i.e., $C = \alpha T^2$. Theoretically, α can be calculated as $\alpha = 0.586 \text{ J/mol K}^3$ [20], where we have used that $\nu_F \approx 10^3 \text{ m/s}$ and there are six Dirac fermions. This is indeed very close to the experimental value, 0.452 J/mol K^3 . Note that thermal-conductivity (κ) measurements on $\text{YCu}_3\text{-Br}$ failed to detect a non-zero $\kappa/T|_{T \rightarrow 0 \text{ K}}$ under magnetic fields [42], which does not seem to agree with the existence of spinon Fermi surfaces induced by a field. However, as $\kappa = (1/3)C\nu_F l$, a very large mean free path l ($> 30 \text{ \mu m}$) is required for the spinons to be detected by the heat-transport measurement ($\kappa/T > 0.01 \text{ mW/K}^2 \text{ cm}$). Such a large value of l is apparently hard to achieve considering the site disorders in this system [38–40]. Also note that our results clearly show excitations down to 0.06 meV, which is much smaller than the gap value determined by the heat-transport measurement [42], suggesting that the system has a gapless ground state.

The Dirac QSL state in $\text{YCu}_3\text{-Br}$ is not the one predicted in the nearest Heisenberg model, which should ex-

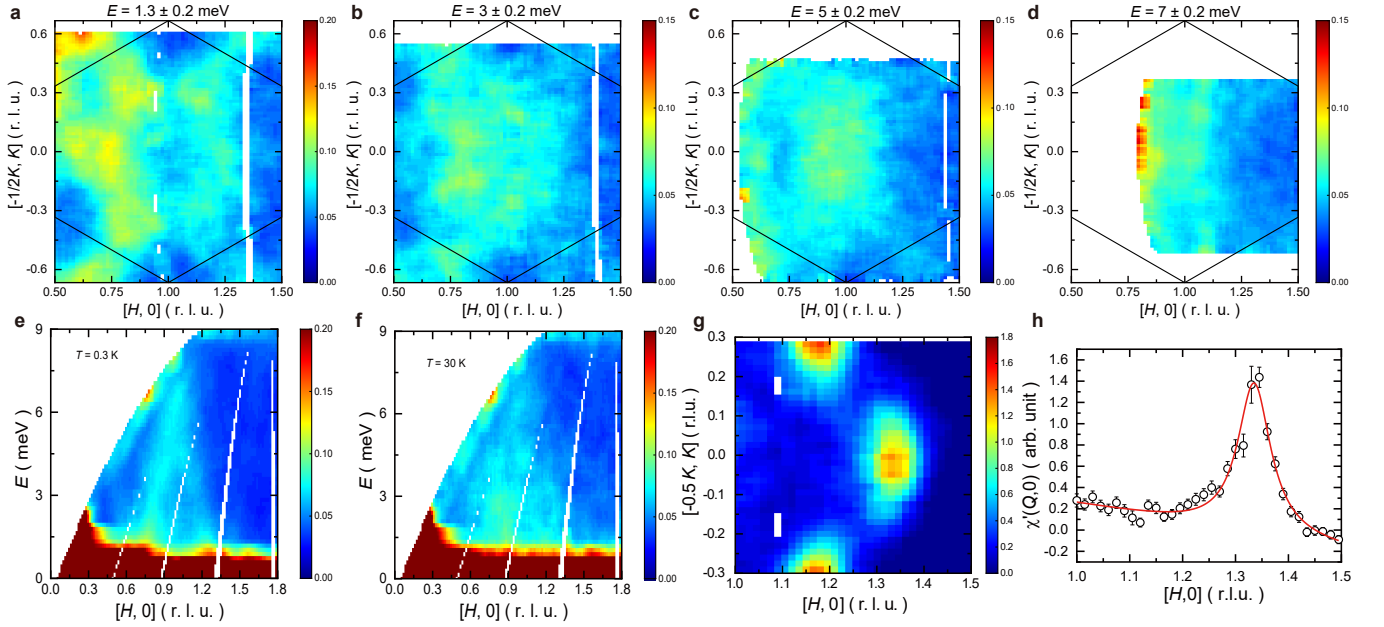


FIG. 4. **High-energy spin excitations at $E_i = 9.986$ meV and static susceptibility $\chi'(Q, 0)$ in $\text{YCu}_3\text{-Br}$.** **a-d**, Intensity contour plots of the INS results at 0.3 K in the $[H, K]$ zone at 1.3 meV (**a**), 3 meV (**b**), 5 meV (**c**) and 7 meV (**d**). **e**, **f**, Intensity contour plots of the INS results as a function of E and Q along the $[H, 0]$ direction at 0.3 K (**e**) and 30 K (**f**). Note that the intensities at small Q near the edge of the colormap (**c-f**) are from the background. **g**, $\chi'(Q, 0)$ at 0.3 K calculated by the Kramers-Kronig relation based on $S(Q, \omega)$ between 0.075 to 8 meV. Only half of the Brillouin zone is shown to avoid the background at lower Q 's. **h**, H dependence of $\chi'(Q, 0)$ around $(4/3, 0)$. The solid line is the fit to the Lorentzian function with a linear background. The error bars represent one-standard-deviation uncertainty in the data based on Poisson statistics with the sample size being the neutron counts.

hibit conical spin excitations at $(0.5, 0)$ (the point M in Fig. 1d) [26]. The position of the spin excitations indicates that the magnetic system may be related to the $Q = (1/3, 1/3)$ phase [49], which suggests that there exist three different nearest exchange J_1 (Fig. 1c). Although this order seems closely related to $\text{Y}_3\text{Cu}_9(\text{OH})_{19}\text{Cl}_8$ [33], which has distorted kagome planes and an enlarged lattice unit cell as shown in Fig. 1c, the kagome lattice remains undistorted in our sample. What is surprising is that the spin excitations close to zero energy are very sharp in our sample, and actually, much sharper than those in the ordered sample [33], which seems to suggest that the emergent Dirac spinons are insensitive to disorder. A detailed discussion on the spectrum of spin wave calculated in the presence of disorder in the form of different J_1 and the contrast with respect to our INS results are given in the Supplementary Information [43]. Whether the melting of the above order can result in a Dirac QSL is an open question. We note that an $1/9$ magnetization plateau and magnetic quantum oscillations have been observed in this system [50], which were explained by a model assuming that a Dirac spinon is coupled with the emergent gauge field, consistent with our observation of conical spin excitations.

Finding a QSL state in the $\text{YCu}_3\text{-Br}$ system seemingly with disorder is surprising, as it is believed that disorder

will typically destroy QSLs [51]. In our case, the disorder is mainly site disorder of Y^{3+} , Br^- , and $(\text{OH})^-$, which results in alternate bonds of the hexagons in the kagome [40]. Note that the undistorted hexagons may also be treated as disorders to the hexagons with alternate bonds, which are related to the $Q = (1/3, 1/3)$ phase [49], depending which quantity of hexagons is larger. Our results show that disorder has negligible effects on the low-energy spin excitations. This is consistent with the observation of magnetic quantum oscillations in this system [50], which typically requires a clean system. This means that the Dirac QSL is either robust against disorder [52, 53] or even induced by disorder [54, 55]. At this stage, an unambiguous theoretical calculation with disorder and longer-range interactions of the dynamic spectrum of frustrated quantum spin models is difficult and subject to certainly approximations such as finite size, finite temperature, finite bond-dimension and so on [56]. On the other hand, the conic spin excitations emerging from Dirac spinons will render the very low-energy spin excitations with a sharp energy-momentum boundary [14, 15, 30, 31], as observed here. Overall, the $\text{YCu}_3\text{-Br}$ system is an interesting platform for further experimental and theoretical studies.

We thank Prof. Yi Zhou, Yuan Li, and Patrick Lee for the discussions. This work is supported by the Na-

tional Key Research and Development Program of China (Grants No. 2022YFA1403400, No. 2021YFA1400401), the K. C. Wong Education Foundation (Grants No. GJTD-2020-01), the Strategic Priority Research Program (B) of the Chinese Academy of Sciences (Grants No. XDB33000000), and the Research Grants Council (RGC) of Hong Kong Special Administrative Region of China (Project Nos. 17301721, AoE/P701/20, 17309822, C7037-22GF, A_HKU703/22 and 17302223). Measurements on AMATERAS were performed based on the approved proposal No. 2022B0048. The measurement on CAMEA was carried out under the proposal number 20220991. We thank HPC2021 system under the Information Technology Services and the Blackbody HPC system at the Department of Physics, University of Hong Kong, as well as the Beijing PARATERA Tech CO.,Ltd. (URL: <https://cloud.paratera.com>).

* kenji.nakajima@j-parc.jp

† zymeng@hku.hk

‡ slli@iphy.ac.cn

- [1] L. Balents, Spin liquids in frustrated magnets, *Nature* **464**, 199 (2010).
- [2] L. Savary and L. Balents, Quantum spin liquids: A review, *Rep. Prog. Phys.* **80**, 016502 (2017).
- [3] Y. Zhou, K. Kanoda, and T.-K. Ng, Quantum spin liquid states, *Rev. Mod. Phys.* **89**, 025003 (2017).
- [4] C. Broholm, R. J. Cava, S. A. Kivelson, D. G. Nocera, M. R. Norman, and T. Senthil, Quantum spin liquids, *Science* **367**, 263 (2020).
- [5] S. A. Kivelson, D. S. Rokhsar, and J. P. Sethna, Topology of the resonating valence-bond state: Solitons and high- T_c superconductivity, *Phys. Rev. B* **35**, 8865 (1987).
- [6] X. G. Wen, Mean-field theory of spin-liquid states with finite energy gap and topological orders, *Phys. Rev. B* **44**, 2664 (1991).
- [7] X.-G. Wen, Colloquium: Zoo of quantum-topological phases of matter, *Rev. Mod. Phys.* **89**, 041004 (2017).
- [8] G.-Y. Sun, Y.-C. Wang, C. Fang, Y. Qi, M. Cheng, and Z. Y. Meng, Dynamical signature of symmetry fractionalization in frustrated magnets, *Phys. Rev. Lett.* **121**, 077201 (2018).
- [9] Y.-C. Wang, M. Cheng, W. Witczak-Krempa, and Z. Y. Meng, Fractionalized conductivity and emergent self-duality near topological phase transitions, *Nature Communications* **12**, 5347 (2021).
- [10] A. Chatterjee, W. Ji, and X.-G. Wen, Emergent generalized symmetry and maximal symmetry-topological-order (2022), [arXiv:2212.14432](https://arxiv.org/abs/2212.14432).
- [11] A. K. Geim and K. S. Novoselov, The rise of graphene, *Nat. Mater.* **6**, 183 (2007).
- [12] M. Z. Hasan and C. L. Kane, Colloquium: Topological insulators, *Rev. Mod. Phys.* **82**, 3045 (2010).
- [13] O. Vafek and A. Vishwanath, Dirac fermions in solids: From High- T_c cuprates and graphene to topological insulators and Weyl semimetals, *Annu. Rev. Condens. Matter Phys.* **5**, 83 (2014).
- [14] Y. Q. Qin, Y.-Y. He, Y.-Z. You, Z.-Y. Lu, A. Sen, A. W. Sandvik, C. Xu, and Z. Y. Meng, Duality between the deconfined quantum-critical point and the bosonic topological transition, *Phys. Rev. X* **7**, 031052 (2017).
- [15] N. Ma, G.-Y. Sun, Y.-Z. You, C. Xu, A. Vishwanath, A. W. Sandvik, and Z. Y. Meng, Dynamical signature of fractionalization at a deconfined quantum critical point, *Phys. Rev. B* **98**, 174421 (2018).
- [16] X. Y. Xu, Y. Qi, L. Zhang, F. F. Assaad, C. Xu, and Z. Y. Meng, Monte carlo study of lattice compact quantum electrodynamics with fermionic matter: The parent state of quantum phases, *Phys. Rev. X* **9**, 021022 (2019).
- [17] X.-Y. Song, C. Wang, A. Vishwanath, and Y.-C. He, Unifying description of competing orders in two-dimensional quantum magnets, *Nat. Commun.* **10**, 4254 (2019).
- [18] S. Sachdev, Kagomé and triangular-lattice Heisenberg antiferromagnets: Ordering from quantum fluctuations and quantum-disordered ground states with unconfined bosonic spinons, *Phys. Rev. B* **45**, 12377 (1992).
- [19] M. B. Hastings, Dirac structure, RVB, and Goldstone modes in the kagomé antiferromagnet, *Phys. Rev. B* **63**, 014413 (2000).
- [20] Y. Ran, M. Hermele, P. A. Lee, and X.-G. Wen, Projected-wave-function study of the spin-1/2 heisenberg model on the kagomé lattice, *Phys. Rev. Lett.* **98**, 117205 (2007).
- [21] M. Hermele, Y. Ran, P. A. Lee, and X.-G. Wen, Properties of an algebraic spin liquid on the kagome lattice, *Phys. Rev. B* **77**, 224413 (2008).
- [22] Y. Iqbal, F. Becca, and D. Poilblanc, Projected wave function study of \mathbb{Z}_2 spin liquids on the kagome lattice for the spin- $\frac{1}{2}$ quantum Heisenberg antiferromagnet, *Phys. Rev. B* **84**, 020407 (2011).
- [23] Y. Iqbal, D. Poilblanc, and F. Becca, Vanishing spin gap in a competing spin-liquid phase in the kagome heisenberg antiferromagnet, *Phys. Rev. B* **89**, 020407 (2014).
- [24] Y.-C. He, M. P. Zaletel, M. Oshikawa, and F. Pollmann, Signatures of dirac cones in a dmrg study of the kagome heisenberg model, *Phys. Rev. X* **7**, 031020 (2017).
- [25] H. J. Liao, Z. Y. Xie, J. Chen, Z. Y. Liu, H. D. Xie, R. Z. Huang, B. Normand, and T. Xiang, Gapless spin-liquid ground state in the $s = 1/2$ kagome antiferromagnet, *Phys. Rev. Lett.* **118**, 137202 (2017).
- [26] W. Zhu, S. shu Gong, and D. N. Sheng, Identifying spinon excitations from dynamic structure factor of spin-1/2 Heisenberg antiferromagnet on the Kagome lattice, *Proc. Natl. Acad. Sci. U.S.A.* **116**, 5437 (2019).
- [27] Z. Zhu, P. A. Maksimov, S. R. White, and A. L. Chernyshev, Topography of spin liquids on a triangular lattice, *Phys. Rev. Lett.* **120**, 207203 (2018).
- [28] Z.-X. Liu and B. Normand, Dirac and chiral quantum spin liquids on the honeycomb lattice in a magnetic field, *Phys. Rev. Lett.* **120**, 187201 (2018).
- [29] S. Hu, W. Zhu, S. Eggert, and Y.-C. He, Dirac spin liquid on the spin-1/2 triangular Heisenberg antiferromagnet, *Phys. Rev. Lett.* **123**, 207203 (2019).
- [30] X.-Y. Song, Y.-C. He, A. Vishwanath, and C. Wang, From spinon band topology to the symmetry quantum numbers of monopoles in Dirac spin liquids, *Phys. Rev. X* **10**, 011033 (2020).
- [31] Y. Nomura and M. Imada, Dirac-type nodal spin liquid revealed by refined quantum many-body solver using neural-network wave function, correlation ratio, and level spectroscopy, *Phys. Rev. X* **11**, 031034 (2021).
- [32] Y. Da Liao, X. Y. Xu, Z. Y. Meng, and Y. Qi, Dirac

- fermions with plaquette interactions. II. SU(4) phase diagram with Gross-Neveu criticality and quantum spin liquid, *Phys. Rev. B* **106**, 115149 (2022).
- [33] D. Chatterjee, P. Puphal, Q. Barthélemy, J. Willwater, S. Süllow, C. Baines, S. Petit, E. Ressouche, J. Olivier, K. M. Zoch, C. Krellner, M. Parzer, A. Riss, F. Garmroudi, A. Pustogow, P. Mendels, E. Kermarrec, and F. Bert, From spin liquid to magnetic ordering in the anisotropic kagome Y-kapellasite $\text{Y}_3\text{Cu}_9(\text{OH})_{19}\text{Cl}_8$: A single-crystal study, *Phys. Rev. B* **107**, 125156 (2023).
- [34] T. H. Han, J. S. Helton, S. Chu, D. G. Nocera, J. A. Rodriguez-Rivera, C. Broholm, and Y. S. Lee, Fractionalized excitations in the spin-liquid state of a kagome-lattice antiferromagnet, *Nature* **492**, 406 (2012).
- [35] Y. Shen, Y.-D. Li, H. Wo, Y. Li, S. Shen, B. Pan, Q. Wang, H. C. Walker, P. Steffens, M. Boehm, Y. Hao, D. L. Quintero-Castro, L. W. Harriger, M. D. Frontzek, L. Hao, S. Meng, Q. Zhang, G. Chen, and J. Zhao, Evidence for a spinon Fermi surface in a triangular-lattice quantum-spin-liquid candidate, *Nature* **540**, 559 (2016).
- [36] L. Ding, P. Manuel, S. Bachus, F. Gruber, P. Gegenwart, J. Singleton, R. D. Johnson, H. C. Walker, D. T. Adroja, A. D. Hillier, and A. A. Tsirlin, Gapless spin-liquid state in the structurally disorder-free triangular antiferromagnet NaYbO_2 , *Phys. Rev. B* **100**, 144432 (2019).
- [37] M. M. Bordelon, C. Liu, L. Posthuma, P. M. Sarte, N. P. Butch, D. M. Pajerowski, A. Banerjee, L. Balents, and S. D. Wilson, Spin excitations in the frustrated triangular lattice antiferromagnet NaYbO_2 , *Phys. Rev. B* **101**, 224427 (2020).
- [38] X.-H. Chen, Y.-X. Huang, Y. Pan, and J.-X. Mi, Quantum spin liquid candidate $\text{YCu}_3(\text{OH})_6\text{Br}_2[\text{Br}_x(\text{OH})_{1-x}]$ ($x \approx 0.51$): With an almost perfect kagomé layer, *J. Magn. Magn. Mater.* **512**, 167066 (2020).
- [39] Z. Zeng, X. Ma, S. Wu, H.-F. Li, Z. Tao, X. Lu, X.-h. Chen, J.-X. Mi, S.-J. Song, G.-H. Cao, G. Che, K. Li, G. Li, H. Luo, Z. Y. Meng, and S. Li, Possible dirac quantum spin liquid in the kagome quantum antiferromagnet $\text{YCu}_3(\text{OH})_6\text{Br}_2[\text{Br}_x(\text{OH})_{1-x}]$, *Phys. Rev. B* **105**, L121109 (2022).
- [40] J. Liu, L. Yuan, X. Li, B. Li, K. Zhao, H. Liao, and Y. Li, Gapless spin liquid behavior in a kagome heisenberg antiferromagnet with randomly distributed hexagons of alternate bonds, *Phys. Rev. B* **105**, 024418 (2022).
- [41] F. Lu, L. Yuan, J. Zhang, B. Li, Y. Luo, and Y. Li, The observation of quantum fluctuations in a kagome Heisenberg antiferromagnet, *Commun. Phys.* **5**, 272 (2022).
- [42] X. Hong, M. Behnami, L. Yuan, B. Li, W. Brenig, B. Büchner, Y. Li, and C. Hess, Heat transport of the kagome heisenberg quantum spin liquid candidate $\text{YCu}_3(\text{OH})_{6.5}\text{Br}_{2.5}$: Localized magnetic excitations and a putative spin gap, *Phys. Rev. B* **106**, L220406 (2022).
- [43] In this Supplemental Information, we include more information of the INS experiment, and the calculation of the linear spin wave analysis for Heisenberg model on kagome lattice..
- [44] Z. Zhu, P. A. Maksimov, S. R. White, and A. L. Chernyshev, Disorder-induced mimicry of a spin liquid in YbMgGaO_4 , *Phys. Rev. Lett.* **119**, 157201 (2017).
- [45] I. Kimchi, A. Nahum, and T. Senthil, Valence bonds in random quantum magnets: Theory and application to YbMgGaO_4 , *Phys. Rev. X* **8**, 031028 (2018).
- [46] Z. Ma, Z.-Y. Dong, J. Wang, S. Zheng, K. Ran, S. Bao, Z. Cai, Y. Shangguan, W. Wang, M. Boehm, P. Steffens, L.-P. Regnault, X. Wang, Y. Su, S.-L. Yu, J.-M. Liu, J.-X. Li, and J. Wen, Disorder-induced broadening of the spin waves in the triangular-lattice quantum spin liquid candidate YbZnGaO_4 , *Phys. Rev. B* **104**, 224433 (2021).
- [47] T. Shimokawa, K. Watanabe, and H. Kawamura, Static and dynamical spin correlations of the $S = \frac{1}{2}$ random-bond antiferromagnetic heisenberg model on the triangular and kagome lattices, *Phys. Rev. B* **92**, 134407 (2015).
- [48] T.-H. Han, M. R. Norman, J.-J. Wen, J. A. Rodriguez-Rivera, J. S. Helton, C. Broholm, and Y. S. Lee, Correlated impurities and intrinsic spin-liquid physics in the kagome material herbertsmithite, *Phys. Rev. B* **94**, 060409 (2016).
- [49] M. Hering, F. Ferrari, A. Razpopov, I. I. Mazin, R. Valentí, H. O. Jeschke, and J. Reuther, Phase diagram of a distorted kagome antiferromagnet and application to Y-kapellasite, *npj Comput. Mater.* **8**, 10 (2022).
- [50] G. Zheng, Y. Zhu, K.-W. Chen, B. Kang, D. Zhang, K. Jenkins, A. Chan, Z. Zeng, A. Xu, O. A. Valenzuela, J. Blawat, J. Singleton, P. A. Lee, S. Li, and L. Li, Unconventional magnetic oscillations in kagome Mott insulators (2023), arXiv:2310.07989.
- [51] S. Dey, Destabilization of U(1) Dirac spin liquids on two-dimensional nonbipartite lattices by quenched disorder, *Phys. Rev. B* **102**, 235165 (2020).
- [52] K. Yang, D. Varjas, E. J. Bergholtz, S. Morampudi, and F. Wilczek, Exceptional dynamics of interacting spin liquids, *Phys. Rev. Res.* **4**, L042025 (2022).
- [53] U. F. P. Seifert, J. Willsher, M. Drescher, F. Pollmann, and J. Knolle, Spin-Peierls instability of the U(1) Dirac spin liquid (2023), arXiv:2307.12295.
- [54] L. Savary and L. Balents, Disorder-induced quantum spin liquid in spin ice pyrochlores, *Phys. Rev. Lett.* **118**, 087203 (2017).
- [55] R. Sibille, E. Lhotel, M. C. Hatnean, G. J. Nilsen, G. Ehlers, A. Cervellino, E. Ressouche, M. Frontzek, O. Zaharko, V. Pomjakushin, U. Stühr, H. C. Walker, D. T. Adroja, H. Luetkens, C. Baines, A. Amato, G. Balakrishnan, T. Fennell, and M. Kenzelmann, Coulomb spin liquid in anion-disordered pyrochlore $\text{Tb}_2\text{Hf}_2\text{O}_7$, *Nat. Commun.* **8**, 892 (2017).
- [56] N. E. Sherman, M. Dupont, and J. E. Moore, Spectral function of the $J_1 - J_2$ heisenberg model on the triangular lattice, *Phys. Rev. B* **107**, 165146 (2023).